SAND2022-2599J

Long wavelength interband cascade lasers

J. A. Massengale[1,2], Yixuan Shen[1], Rui Q. Yang[1,*], S. D. Hawkins[3], and J. F. Klem[3]

[1]School of Electrical and Computer Engineering, University of Oklahoma, Norman, OK 73019, USA
[2]Homer L. Dodge Department of Physics and Astronomy, University of Oklahoma, Norman, OK 73019, USA
[3]Sandia National Laboratories, PO Box 5800, Albuquerque, NM, USA 87185-1085

*email: Rui.q.Yang@ou.edu

Sandia National Laboratories is a multimission laboratory managed and operated by National Technology & Engineering Solutions of Sandia, LLC, a wholly owned subsidiary of Honeywell International Inc., for the U.S. Department of Energy's National Nuclear Security Administration under contract DE-NA0003525.

Abstract

InAs-based interband cascade lasers (ICLs) can be more easily adapted toward long wavelength operation than their GaSb counterparts. Devices made from two recent ICL wafers with an advanced waveguide structure are reported, which demonstrate improved device performance in terms of reduced threshold current densities for ICLs near 11 μm or extended operating wavelength beyond 13 μm. The ICLs near 11 μm yielded a significantly reduced continuous wave (cw) lasing threshold of 23 A/cm^2 at 80 K with substantially increased cw output power, compared with previously reported ICLs at similar wavelengths. ICLs made from the second wafer incorporated an innovative quantum well (QW) active region, comprised of InAsP layers, and lased in pulsed-mode up to 120 K at 13.2 μm, the longest wavelength achieved for III-V interband lasers.

Index Terms—III-V materials, advanced waveguide, Interband cascade laser (ICL), long wavelength operation, mid-IR laser, semiconductor laser.

In the decades since the original proposal of the interband cascade laser (ICL) [1], a multitude of developments have paved the way for this III-V based technology to yield efficient and coherent mid-IR sources [2-5]. Operating in a wide range of wavelengths from below 3 μm to above 11 μm, ICLs based on the type-II quantum well (QW) active region boast many technological applications including gas/chemical sensing, imaging, and industrial process control [6-8].

While type-II ICLs, grown mostly on GaSb substrates, have demonstrated efficient room temperature operation in the 3-6 μm range [5], two key questions remain: 1) Can the ICL support longer wavelength operation with low threshold current densities, and 2) Just how far into the longer wavelength regime can the ICL technology be pushed? It should be noted that extension to longer wavelengths is challenging for the mature GaSb-based ICLs [2-5]. This is primarily due to the InAs/AlSb superlattice (SL) needed to form the optical cladding layers. Such a SL would need to be significantly thicker to accommodate the longer optical wave decay length, which complicates the molecular beam epitaxy (MBE) growth. Additionally, the SL has a low thermal conductivity, and so an increase in the overall SL thickness would cause the thermal resistance of the device to increase accordingly, hindering performance.

One solution to alleviate such concerns is to, instead, grow ICL structures on InAs substrates and replace the InAs/AlSb SL cladding with n^+-doped InAs plasmon enhanced cladding in combination with undoped InAs separate confinement layers (SCLs) [9-12]. This InAs-based approach [4] enabled pulsed lasing up to 55 °C near 7.1 μm [13] and extended the ICL operation to 11.1 μm [14], the longest wavelength at the time among III-V interband lasers. However, the threshold current density (J_{th}) of the latter, long wavelength device, was relatively high (e.g., 95 A/cm^2 at 80 K in cw mode near 10.8 μm) and operated only up to 97 and 130 K in cw and pulsed modes, respectively. This relatively modest device performance can be improved significantly by using an advanced waveguide configuration, which was later developed for InAs-based ICLs operating near 4.6 μm [15]. By introducing an intermediate SL cladding layer between the SCL and the plasmon cladding layer, the advanced waveguide configuration can enhance the optical confinement and simultaneously reduce the optical loss, resulting in a low J_{th}. It should be noted that the plasmon enhanced waveguide ICLs can also be achieved on GaSb substrates with heavily doped n^+-InAsSb layers and GaSb SCLs [16-17] at the cost of more complicated carrier transport and MBE growth [4].

In this work, we report the recent study of InAs-based ICLs with the advanced waveguide structure for long wavelength operation. Devices from one structure showed significantly reduced threshold current densities compared to previous ICLs at similar wavelengths near 11 μm. Devices from the second structure extended the lasing wavelength of ICLs longer than 13 μm with an innovative QW active region comprised of InAsP layers based on the relevant perspective on band-edge positions in type-II heterostructures [18], which discussed a method to address the issue of a reduced wavefunction overlap for photon emission at long wavelengths with spatially indirect transitions in a type-II QW.

Two sets of 20-stage ICLs were grown on InAs substrates, both including the advanced waveguide design, where the layer thicknesses of the intermediate SL cladding and InAs SCL layers were 1.65 μm and 0.83 μm, respectively. The bottom n^+-InAs plasmon cladding layer thickness was 2 μm, while the top was 1.1 μm. The doping level of the plasmon cladding was 3.2×10^{18} cm^{-2}, which was lowered by approximately 54% compared with ref. [14], to reduce optical losses due to free carrier absorption.

In addition to adapting the advanced waveguide for both ICLs, the second ICL had a modified active region compared with the first, in order to enhance its

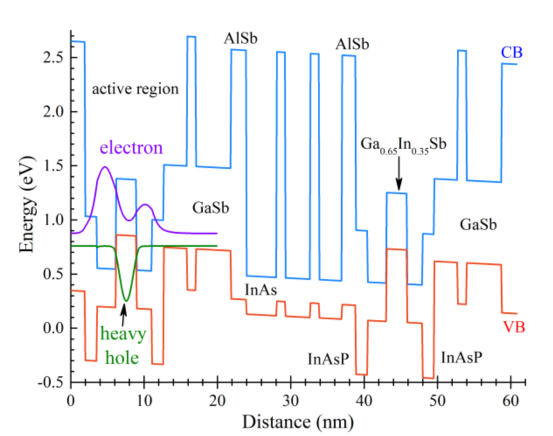

Fig. 1. Illustrated band-edge diagram of one cascade stage and the layer sequence for the 2nd ICL wafer.

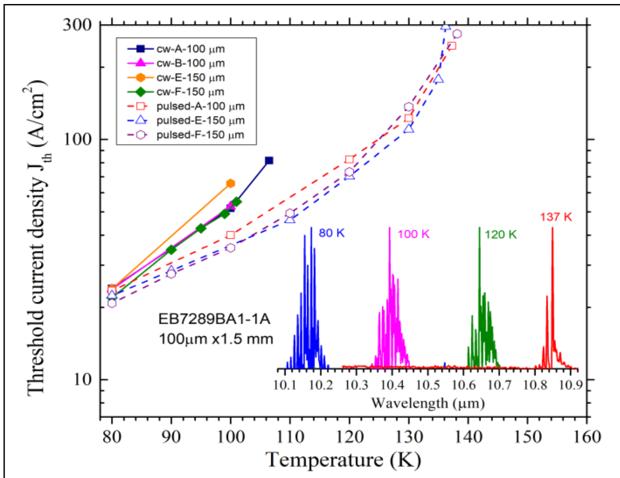

Fig. 2. Threshold current density (J_{th}) as a function of temperature (T) for several devices made from the first ICL wafer. The inset depicts the pulsed lasing spectrum for device EB7289BA1-1A at various temperatures.

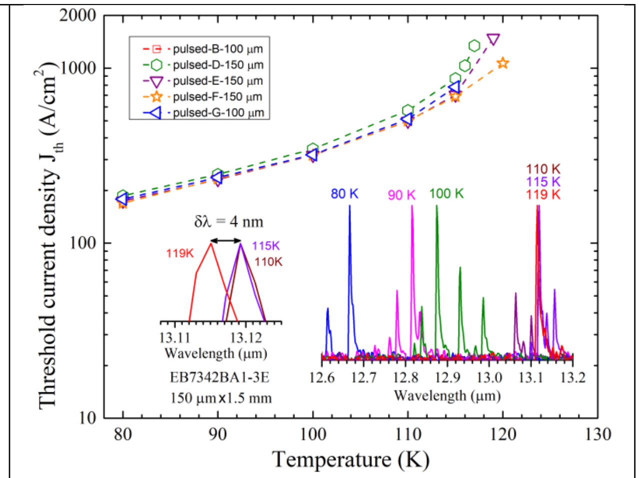

Fig. 3. J_{th} as a function of T for several devices from the 2nd ICL wafer. The right inset shows the pulsed lasing spectrum for EB7342BA1-3E, while the left inset shows a zoomed in view depicting the blue shift of 4 nm.

long wavelength operation. In the first ICL wafer (EB7289), a typical AlSbAs/InAs/$Ga_{0.65}In_{0.35}Sb$/InAs/AlSbAs W-shape QW active region was employed with layer thicknesses of 23/34.5/28/31.5/12 Å in the growth direction. When extending operation to longer wavelengths, a thicker InAs layer is needed, which leads to a reduced electron-hole wavefunction overlap in this type-II QW as the electrons and holes are mainly localized at different layers. This could cause the optical gain (generated from the spatially indirect interband transition in the type-II QW) to be insufficient to overcome the increased loss at a long wavelength and thus render the lasing unreachable. But as pointed out in Ref [18], the energy level of an electronic state in a QW could be moved down by using a barrier layer with a low valence band-edge, resulting in a lower interband transition energy for photon emission at longer wavelengths. Phosphorus containing compounds are such a barrier material that can lower the electron energy level for longer wavelength emission without increasing the InAs layer thickness. So, for the second ICL wafer (EB7342), a modified active region consisting of a AlSbAs/$InAs_{0.5}P_{0.5}$/InAs/$Ga_{0.65}In_{0.35}Sb$/InAs/$InAs_{0.5}P_{0.5}$ QW was grown, with layer thicknesses of 19/16/26.5/28/21.5/16 Å, respectively, where the InAs layer thicknesses were substantially reduced (*e.g.*, 26.5 vs. 34.5) compared to that in the first ICL wafer. The band-edge diagram of one cascade stage along with the layer sequence for the 2nd ICL wafer is given in Fig. 1, which is a qualitative illustration rather than an exact description considering that there exist some uncertainties and variations in material parameters due to several factors such as interfacial compositions and strains.

The grown wafers were fabricated into 100-μm-wide (EB7289BA1-1A and EB7342BA1-3G) and 150-μm-wide (EB7289BA1-1E and EB7342BA1-3F and 3E) broad area (BA) mesas using wet chemical etching. The wafers were left un-thinned and cleaved into 1.5-mm-long laser bars without facet coating, which were mounted epi-side up on copper heat sinks for testing.

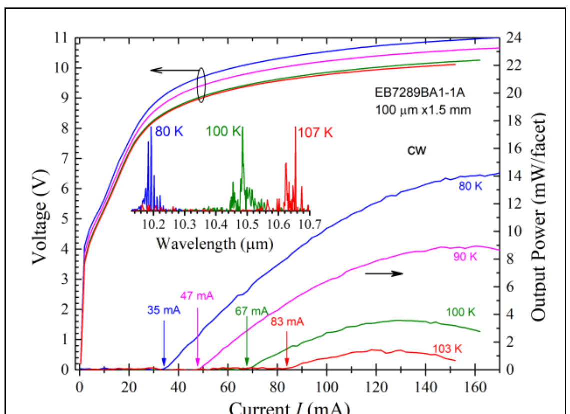

Fig. 4. Current-voltage- and output power characteristics for EB7289BA1-1A in cw mode, where arrows indicate threshold at various temperatures. The inset shows the cw emission spectra between 80 K and 107 K.

Multiple devices from EB7289 were able to operate in cw mode above 100 K, and in pulsed-mode above 130 K with lasing wavelengths near 11 μm, as shown in Fig. 2. The devices from EB7342 were only able to operate in pulsed mode (1 μs pulse width and 5 kHz repetition rate) at temperatures up to 120 K at wavelengths beyond 13 μm as shown in Fig. 3 (and the inset in Fig. 6), which is the longest ever reported among III-V interband lasers. This verified the theoretical prediction [18] that P-containing barrier layers could lower the electronic energy level in a QW with reduced InAs layer thicknesses.

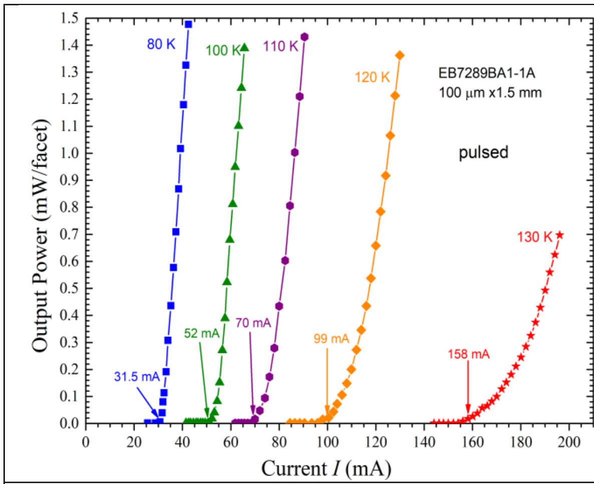

Fig. 5. Pulsed output power as a function of injection current at several temperatures for EB7289BA1-1A.

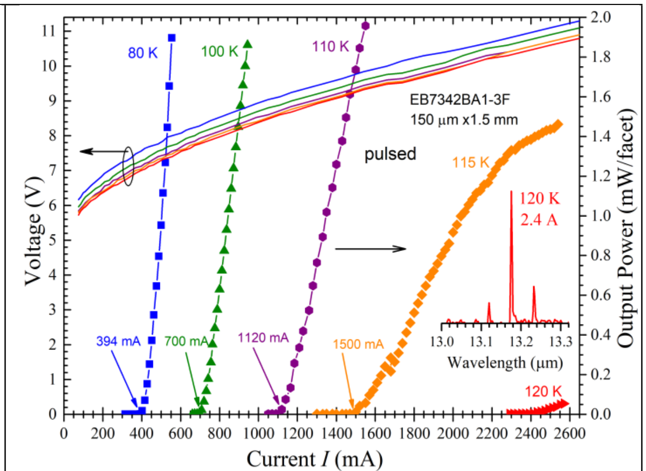

Fig. 6. Pulsed current-voltage- and output power characteristics at several temperatures for EB7342BA1-3F. The inset is its lasing spectrum at 120 K.

In cw mode, a representative device from the first ICL wafer, EB7289BA1-1A, lased at 10.2 μm at 80 K and operated up to 107 K at an emission wavelength of 10.65 μm as shown in the inset in Fig. 4. At 80 K, the J_{th} was ~23 A/cm^2, which is a reduction of about four times compared with the previously reported 20-stage ICL with a similar wavelength described in Ref. [14], but 2.3 times that of a 15-stage ICL emitting at 9 μm at 80 K [19]. The threshold voltage (V_{th}) of this device was 9.2 V at 80 K, which is significantly higher than the typical value (3.9 V [14]) of previous 20-stage ICLs. The abnormally high V_{th} could be caused by a possible problem in the carrier transport, which is not understood at this moment. The high V_{th} and the corresponding possible issue in carrier transport limited the maximum cw and pulsed operating temperatures, which is reflected by the maximum allowable threshold current density (82 A/cm^2 in cw and <300 A/cm^2 in a pulsed mode) as shown in Fig. 2. This suggests there is significant room for improvement for ICLs at this long wavelength. On the other hand, the cw output power for this device was 14.3 mW/facet with an injection current of 172 mA at 80 K, which is an increase of approximately four times compared with that for the ICL in Ref. [14] and comparable to that (15 mW for the 9 μm ICL at 200 mA) discussed in Ref. [19]. Appreciable output power was obtained at temperatures up to 103 K as shown in Fig. 4. Actual output power should be somewhat higher because the measurement does not account for beam divergence loss. Several devices from wafer EB7289 exhibited similar output powers. The increase in output power from these devices clearly indicates that the optical internal loss is reduced in the advanced waveguide configuration compared to previous ICLs with only plasmon cladding layers.

Under pulsed operation, EB7289BA1-1A was able to operate up to 137 K at a wavelength of 10.85 μm, as shown in the inset in Fig. 2, a slightly higher temperature than that in Ref. [14], with a J_{th} of 245 A/cm^2. As shown in Fig. 5, the slope efficiency was nearly insensitive to temperature from 80 to 110 K. The extracted external quantum efficiency (EQE) reached ~290% at 80 K, indicating the cascaded emission of photons in the ICL, and dropped to ~60% at 130 K. According to the optical properties and threshold current densities, this laser should be capable of operating well above 130 K. The fact that the lasing was only up to 137 K suggests possible issues beyond the optical properties, which need to be investigated in the future.

A representative device from the second ICL wafer, EB7342BA1-3G, lased at a wavelength of 12.7 μm in pulsed mode at 80 K, albeit with a large J_{th} of 179 A/cm^2. The maximum operating temperature for this device was 115 K, at a lasing wavelength of 13.23 μm, which represents a new record for long wavelength operation among III-V interband lasers. Also, three more devices from this wafer (EB7342BA1-3E, 3D and 3F) were able to lase at slightly higher temperatures of 119, 117 and 120 K, respectively. However, the lasing wavelength for device 3E at 119 K was shorter, at 13.11 μm (similarly for device 3D). This is due to the band filling effect, as shown in the insets in Fig. 3 (for device 3E), which can occur in mid-IR lasers and placed an upper wavelength limit of 9.5 μm for optically pumped Sb-based type-II QW lasers [20]. The effect occurs because as the lasing emission is pushed toward longer wavelengths with increasing temperature, the waveguide loss rapidly increases and there also tends to be a reduced modal overlap with the gain medium. Taken together, these effects cause an increase in threshold current density and the number of carriers at higher energy states, which shifts the peak optical gain to a higher energy, resulting in the blue-shift of lasing wavelength rather than a red-shift with narrowing bandgap when temperature is increased. This blue shift effect is also a limiting factor for the longer wavelength operation because one cannot simply increase optical gain to reach the threshold with a high current injection. The observed blue-shift for device EB7342BA1-3E from 115 to 119 K is approximately 4 nm, as indicated in the inset of Fig 3.

Compared with devices from EB7289, those from EB7342 consistently lased with significantly higher threshold current densities, and only in pulsed-mode operation, though they have the same waveguide structure with identical doping profile. The threshold voltage for devices made from the second ICL wafer was ~7.5 V at 80 K and increased at higher temperatures due to the rapid increase of threshold current as shown in Fig. 6, which is also higher than what is typically expected and implies similar issues as in devices from wafer EB7289. Nevertheless, devices from EB7342 sustain lasing at higher threshold current densities (>1000 A/cm^2) as shown in Fig. 3. This suggests that possible issues related to carrier transport might be less severe in EB7342, which is also reflected by a lower voltage (~6 V) at 75 mA as shown in Fig. 6 compared to that (>9 V in Fig. 4) in devices made from EB7289. Considering that the transparency carrier density is usually low at low temperatures [21] and devices from EB7342 lased at substantially longer wavelengths with a modified active QW region, the higher threshold current density may be mainly related to high optical internal loss due to more free-carrier absorption and other mechanisms such as intersubband transitions in QWs. To examine this, the peak output power as a function of injection current (I) for device EB7342BA1-3F was measured and shown in Fig. 6. The extracted EQE was 41% at 80 K, 18% at 100 K, 12% at 110 K, 5.3% at 115 K and 0.67% at 120K, which are much lower than that obtained from device EB7289BA1-1A. This suggests that high internal absorption loss is a major cause for the higher threshold current density in devices made from wafer EB7342. Nevertheless, the innovative QW active region produced a sufficient gain at a moderate threshold current density to overcome the increased absorption loss at such a long wavelength. Although this innovative QW architecture is in its infancy with some unexplored aspects, it may open up a promising approach to further improve ICL device performance in the long wavelength region.

In summary, InAs-based ICLs have been demonstrated with improved device performance at emission wavelengths near 11 μm. Furthermore, a modified QW active region has been implemented into an ICL structure and enabled ICL operation beyond 13 μm, which have initially proved our theoretical prediction [18] and paved the way to further exploration of ICLs in the long wavelength region. For a wide range of practical applications, these long wavelength ICLs need to be capable of operating at room temperature. Possible issues are identified, which suggest significant room for further improvements toward that goal. We believe that with more effort, ICLs should be able to perform better in an extended wavelength region and at elevated temperatures.

ACKNOWLEDGMENT

The work at the University of Oklahoma was partially supported by NSF (ECCS-1931193). This work was performed, in part, at the Center for Integrated Nanotechnologies, an Office of Science User Facility operated for the U.S. Department of Energy (DOE) Office of Science. Sandia National Laboratories is a multimission laboratory managed and operated by National Technology & Engineering Solutions of Sandia, LLC, a wholly owned subsidiary of Honeywell International, Inc., for the U.S. DOE's National Nuclear Security Administration under contract DE-NA-0003525. The views expressed in the article do not necessarily represent the views of the U.S. DOE or the United States Government. We thank Lance McDowell and Zhisheng Shi for lending a MCT detector and help in getting the MCT detector response spectrum.

Data Availability Statement

The data that support the findings of this study are available from the corresponding author upon reasonable request.

REFERENCES

[1] R. Q. Yang, "Infrared laser based on intersubband transitions in quantum wells", *Superlattices Microstruct.*, **17**, 77 (1995).

[2] R. Q. Yang, "Interband Cascade (IC) Lasers," in *Semiconductor Lasers fundamentals and applications*, edited by A. Baranov and E. Tournie, Cambridge, UK: Woodhead Publishing, 2013, ch. 12, pp. 487-513.

[3] J. Koeth, R. Weih, J. Scheuermanna, M. Fischera, A. Schadeb, M. Kamp, S. Höfling, "Mid infrared DFB interband cascade lasers", Proc. SPIE, **10403**, 1040308 (2017).

[4] R. Q. Yang, L. Li, W. Huang, S. M. Shazzad Rassel, J. A. Gupta, A. Bezinger, X. Wu, G. Razavipour, and G. C. Aers, "InAs-based interband cascade lasers", *IEEE J. Sel. Top. Quant. Electron*., **25**, 1200108 (2019).

[5] J. R. Meyer, W. W. Bewley, C. L. Canedy, C. S. Kim, M. Kim, C. D. Merritt, and I. Vurgaftman, "The interband cascade laser", *Photonics*, **7**, 75 (2020).

[6] I. Vurgaftman, P. Geiser, W. W. Bewley, C. D. Merritt, C. L. Canedy, M. V. Warren, M. Kim, C. S. Kim, J. R. Meyer, "Sensitive Chemical Detection with Distributed Feedback Interband Cascade Lasers," In *Encyclopedia of Analytical Chemistry*, Meyers, R.A., Ed.; Wiley: Chichester, UK, 2016.

[7] M. Von Edlinger, J. Scheuermann, R. Weih, L. Nähle, M. Fischer, J. Koeth, S. Höfling, M. Kamp, "Interband Cascade Lasers for Applications in Process Control and Environmental Monitoring," *Light Energy Environ. Congr.* **2015**, *EM2A*, 5.

[8] C. S. Goldenstein, R. M. Spearrin, J. B. Jeffries, R. K. Hanson, "Infrared laser-absorption sensing for combustion gases," *Prog. Energy Combust. Sci.* **2016**, *60*, 132–176.

[9] Z. Tian, R. Q. Yang, T. D. Mishima, M. B. Santos, R. T. Hinkey, M. E. Curtis, and M. B. Johnson, "InAs-based interband cascade lasers near 6 μm", Electron. Lett. **45**, 48 (2009).

[10] Z. Tian, R. Q. Yang, T. D. Mishima, M. B. Santos, M. B. Johnson, "Plasmon-waveguide interband cascade lasers near 7.5 μm" IEEE Photo. Technol. Lett. **21**, 1588 (2009).

[11] R. T. Hinkey, Z. Tian, R. Q. Yang, T. D. Mishima, and M. B. Santos, "Reflectance spectrum of plasmon waveguide interband cascade lasers and observation of the Berreman effect," *J. Appl. Phys*. **110**, 043113 (2011).

[12] R. Q. Yang, L. Li, L. Zhao, Y. Jiang, Z. Tian, H. Ye, R. T. Hinkey, C. Niu, T. D. Mishima, M. B. Santos, J. C. Keay, M. B. Johnson, K. Mansour, "Recent progress in development of InAs-based Interband Cascade Lasers" Proc. SPIE **8640**, paper 86400Q (2013).

[13] M. Dallner, F Hau, S Höfling, M Kamp, "InAs-based interband cascade lasers emitting around 7 μm with threshold current densities below 1 kA/cm^2 at room temperature", Appl. Phys. Lett., **106**, 041108 (2015).

[14] Lu Li, H. Ye, Y. Jiang, R. Q. Yang, J. C. Keay, T. D. Mishima, M. B. Santos, and M. B. Johnson, "MBE-grown long-wavelength interband cascade lasers on InAs substrates", *Journal of Crystal Growth,* **425**, 369 (2015).

[15] L. Li, Y. Jiang, H. Ye, R. Q. Yang, T. D. Mishima, M. B. Santos, and M. B. Johnson, "Low-threshold InAs-based interband cascade lasers operating at high temperatures", *Appl. Phys. Lett*., **106**, 251102 (2015).

[16] C. L. Canedy, M. V. Warren, C. D. Merritt, W. W. Bewley, C. S. Kim, M. Kim, I. Vurgaftman, and J. R. Meyer, "Interband cascade lasers with longer wavelengths", Proc. SPIE, **10111**, 101110G (2017).

[17] Y. Lin, J. A. Massengale, W. Huang, R. Q. Yang, T. D. Mishima, M. B. Santos, "Examination of the Durability of Interband Cascade Lasers Against Structural Variations", J. Infrared & Millimeter Waves. **39**, 137 (2020).

[18] R. Q. Yang, "Electronic States and Interband Tunneling Conditions in Type-II Quantum Well Heterostructures", J. Appl. Phys. **127**, 025705 (2020).

[19] Z. Tian, L. Li, H. Ye, R.Q. Yang, T.D. Mishima, M.B. Santos, and M.B. Johnson, "InAs-based interband cascade lasers with emission wavelengths at 10.4 μm," *Electron. Lett*. **48**, 113–114 (2012).

[20] A. P. Ongstad, R. Kaspi, G. C. Dente, M. L. Tilton, R. Barresi, and J. R. Chavez, "Wavelength tuning limitations in optically pumped type-II antimonide lasers", *Appl. Phys. Lett.*, **92**, 141106 (2008).

[21] Y-M. Mu, R. Q. Yang, "Theoretical investigation of mid-infrared interband cascade lasers based on type II quantum wells," J. Appl. Phys. **84** (1998) 5357-5359.